Factor VIII A3 domain substitution N1922S results in hemophilia A due to domain-specific misfolding and hyposecretion of functional protein

Ryan J. Summers,[1] Shannon L. Meeks,[2] John F. Healey,[2] Harrison C. Brown,[2] Ernest T. Parker,[2] Christine L. Kempton,[2,3] Christopher B. Doering,[2] and Pete Lollar[2]

[1]Emory University School of Medicine, Atlanta, GA; [2]Aflac Cancer Center and Blood Disorders Service, Children's Healthcare of Atlanta and Emory University, Atlanta, GA; and [3]Department of Hematology and Medical Oncology, Emory University, Atlanta, GA

A point mutation leading to amino acid substitution N1922S in the A3 domain of factor VIII (fVIII) results in moderate to severe hemophilia A. A heterologous expression system comparing N1922S-fVIII and wild-type fVIII (wt-fVIII) demonstrated similar specific coagulant activities but poor secretion of N1922S-fVIII. Immunocytochemical analysis revealed that intracellular levels of N1922S-fVIII were similar to those of wt-fVIII. The specific activity of intracellular N1922S-fVIII was 10% of that of wt-fVIII, indicating the presence of large amounts of a nonfunctional N1922S-fVIII–folding intermediate. wt-fVIII colocalized with both endoplasmic reticulum (ER)– and Golgi-resident proteins. In contrast, N1922S-fVIII colocalized only with ER-resident proteins, indicating a block in transit from the ER to the Golgi. A panel of conformation-dependent monoclonal antibodies was used to determine native or nonnative folding of N1922S-fVIII. Intracellular N1922S-fVIII but not secreted N1922S-fVIII displayed abnormal folding in the A3 and C1 domains, indicating that the A1, A2, and C2 domains fold independently into antigenically intact tertiary structures, but that folding is stalled in the mutant A3 and its contiguous C1 domain. In summary, the N1922S substitution results in poor secretion of a functional protein, and the domain-specific defect in folding and intracellular trafficking of N1922S-fVIII is a novel mechanism for secretion defects leading to hemophilia A. (*Blood*. 2011;117(11):3190-3198)

Introduction

Hemophilia A is an X-linked bleeding disorder caused by a deficiency of factor VIII (fVIII). It is classified as mild, moderate, or severe based on plasma fVIII levels of greater than 0.05-0.4 U/mL, 0.01-0.05 U/mL, or less than 0.01 U/mL, respectively.[1] With some exceptions, this classification correlates well with the bleeding diathesis such that patients with mild disease have abnormal bleeding only after trauma or surgery, whereas severe hemophilia A is characterized by spontaneous bleeding into joints or soft tissues.[2]

FVIII is synthesized as an ~ 300-kDa glycoprotein by hepatocytes, liver sinusoidal endothelial cells, and certain types of extrahepatic endothelial cells.[3-6] It contains a domain sequence designated A1-A2-B-*ap*-A3-C1-C2 and circulates as an A1-A2-B/*ap*-A3-C1-C2 heterodimer bound noncovalently to von Willebrand factor (VWF), which protects it from rapid clearance.[7] The homologous ~ 40-kDa A1, A2, and A3 domains are each made up of 2 cupredoxin-like subdomains that form an extensive interface.[8-10] During the activation of fVIII by thrombin to fVIIIa, the B domain and an *ap* activation peptide are released, and cleavage between the A1 and A2 domains produces an A1/A2/A3-C1-C2 fVIIIa heterotrimer.[11] FVIIIa is a cofactor for factor IXa during the proteolytic activation of factor X on relevant phospholipid membrane surfaces. At physiologic concentrations, the A2 subunit spontaneously dissociates, leading to loss of fVIIIa cofactor activity.[12]

Mild and moderate hemophilia A are caused by missense mutations or small deletions in the *F8* gene that lead to decreased expression of a normally functioning fVIII molecule, normal expression of dysfunctional fVIII, or a combination of both. More than 200 mutations that produce mild/moderate hemophilia A have been reported.[2,13,14] Several molecular mechanisms that produce dysfunctional fVIII have been identified, including a decreased ability to bind phospholipid, VWF,[15] or factor IXa[16]; impaired thrombin activation; and abnormally fast A2 subunit dissociation.[17] In contrast, the mechanisms underlying mild/moderate hemophilia A due to low-level secretion of a functional fVIII molecule are less well understood. In this study, we identified a N1922S A3 domain substitution in a patient who produces a functionally normal or near normal fVIII molecule that is expressed poorly. Characterization of this molecule led to the identification of intermediates along the pathway of fVIII biosynthesis in which the mutant A3 domain and its contiguous C1 domain were misfolded.

Methods

Materials

DMEM/F12 (11330-032), fetal bovine serum (FBS), Dulbecco phosphate-buffered saline (DPBS) without calcium or magnesium, AIM V culture medium, penicillin, and streptomycin were purchased from Invitrogen. Cell transfections were performed with Lipofectamine-2000 (Invitrogen). Antibiotic selection was done using geneticin (Invitrogen). Restriction enzymes and Phusion High Fidelity PCR Master Mix were purchased from New England Biolabs. Oligonucleotide primers were purchased from Integrated DNA Technologies. Sulfo-NHS-LC-biotin and M-PER mammalian protein

Submitted September 13, 2010; accepted December 16, 2010. Prepublished online as *Blood* First Edition paper, January 7, 2011; DOI 10.1182/blood-2010-09-307074.

The online version of this article contains a data supplement.

The publication costs of this article were defrayed in part by page charge payment. Therefore, and solely to indicate this fact, this article is hereby marked "advertisement" in accordance with 18 USC section 1734.

extraction reagent were obtained from Pierce Biotechnology. Streptavidin-alkaline phosphatase conjugate was purchased from Jackson ImmunoResearch. Clotting times were measured using a STart coagulation instrument (Diagnostica Stago). Activated partial thromboplastin reagent was purchased from Trinity Biotech. Pooled citrated normal human plasma and fVIII-deficient plasma were obtained from George King Bio-Medical. Ultracel 30000 MWCO centrifugal filter units were obtained from Millipore. Goat anti–mouse alkaline phosphatase-conjugated antibody and Tween 20 were purchased from Bio-Rad. Triton X-100 was purchased from Sigma. RNase A was purchased from QIAGEN. A baby hamster kidney–derived cell line, designated BHK-M,[18] was used for transfection of fVIII cDNAs. Full-length recombinant fVIII, Kogenate FS (Bayer Healthcare), was a gift from Hemophilia of Georgia (Atlanta, GA). Domain-specific anti-fVIII monoclonal antibodies (MAbs) 2-116 (anti-A1), 1D4 (anti-A2), 4A4 (anti-A2), 2-54 (anti-A2), 2-76 (anti-A2), I92 (anti-A3), G38 (anti-A3), 2-113 (anti-A3), I143 (anti-A3), I130 (anti-A3), F147 (anti-A3), 2A9 (anti-C1), I14 (anti-C2), 3E6 (anti-C2), and 2-117 (anti-C2) were purified using previously described procedures,[19] except for MAbs G38 and I143, which were adsorbed to a 2-mL protein G agarose chromatography column (Kirkegaard & Perry Laboratories) and eluted at pH 2.5. MAbs (1 mg/mL in PBS) were biotinylated by the addition of sulfosuccinimidyl-6-(biotinamido) hexanoate to 1 mg/mL and incubation for 30 minutes at 4°C. The biotinylated MAb preparation was exchanged into 0.15M NaCl, 20mM HEPES (N-2-hydroxyethylpiperazine-N′-2-ethanesulfonic acid), pH 7.4 (HBS)/0.05% sodium azide to a final concentration of 0.5 mg/mL by repeated ultrafiltration. All other materials were reagent grade or are described in the cited literature.

Construction of a cDNA encoding B-domain–deleted human N1922S-fVIII

A cDNA encoding wild-type human B-domain–deleted fVIII (BDD wt-fVIII) containing a 14–amino acid segment, SFSQNPPVLKRHQR, in place of the B domain[20] in a mammalian expression plasmid designated ReNeo that encodes geneticin resistance was constructed as described previously.[21] wt-fVIII/ReNeo was used as a template to produce cDNAs encoding N1922S-fVIII and for comparison, V634M-fVIII, using splicing-by-overlap extension mutagenesis,[22] as described in the supplemental data (available on the *Blood* Web site; see the Supplemental Materials link at the top of the online article).

Heterologous expression of fVIII

BHK-M cells were transfected with fVIII cDNA constructs and cultured in the presence of DMEM/F12 containing 10% FBS, 100 units/mL penicillin, 100 μg/mL streptomycin, and 500 μg/mL geneticin for 12 days. Ninety-six geneticin-resistant clones were initially screened for fVIII production using the fVIII antigen assay. The 24 clones exhibiting the highest fVIII antigen level were plated in individual wells on a 24-well plate, grown to at least 80% confluence, and reassayed by ELISA. The top 6 clones were plated on a 6-well plate and 72 hours later were assayed by ELISA. The top 3 fVIII-expressing clones were then divided into 75-cm^2 flasks, grown for 72 hours, and reassayed by ELISA. The top-producing clone was identified and maintained in DMEM/F12 containing 10% FBS, 100 units/mL of penicillin, 100 μg/mL of streptomycin, and 100 μg/mL of geneticin.

BHK-M cells expressing wt-fVIII, N1922S-fVIII, or V634M-fVIII were grown to at least 90% confluence, washed 3 times with 5 mL of DPBS, and switched to serum-free AIM V medium. At 24 hours, the AIM V medium was removed and stored at 4-8°C for fVIII activity and antigen assays. Given the low levels of secretion of the N1922S-fVIII, the medium was concentrated 15-fold by ultrafiltration before storage. The cells were washed once with DPBS, followed by the addition of mammalian protein-extraction reagent (M-PER) and incubated for 5 minutes at room temperature (RT) on a rotator. The lysate was spun at 14 000*g* for 10 minutes, and the supernatant was collected and stored at 4-8°C for fVIII activity and antigen assays.

FVIII activity and antigen assays

FVIII coagulant activity was measured using the activated partial thromboplastin reagent-based one-stage coagulation assay, as described previously[23] except that preincubation of fVIII-deficient plasma and activated partial thromboplastin reagent was conducted for 4 minutes at 37°C. Pooled normal human plasma referenced against a World Health Organization standard was used as the standard. The ability of thrombin to activate wt-fVIII and N1922S-fVIII was determined using a 2-stage coagulation assay in which fVIII is initially reacted with thrombin before addition to fVIII-deficient plasma and activated partial thromboplastin reagent, as described previously.[23] The activation quotient is defined as the ratio of fVIII activity measured by the 2-stage assay divided by the activity measured by the one-stage coagulation assay. FVIII activity also was determined by plasma-free intrinsic fXase assay using purified factor IXa, factor X, and unilamellar phosphatidylcholine/phosphatidylserine vesicles, as described previously.[24,25]

Secreted or intracellular fVIII antigen from BHK-M medium or lysates containing wt-fVIII or N1922S-fVIII was measured by ELISA. MAb 4A4, which binds denatured fVIII as judged by Western blot analysis, was used as the capture antibody, and MAbs 2-116, 1D4, 2-113, G38, I92, 2A9, 2-117, or 3E6 were used as biotinylated secondary antibodies. Bound biotinylated antibodies were detected using streptavidin–alkaline phosphatase conjugate and its substrate, *p*-nitrophenylphosphate, as described previously.[19] For quantitation of fVIII antigen, a separate standard curve for each biotinylated MAb was constructed using purified wt-fVIII.

Immunocytochemical assay of fVIII

Intracellular expression of fVIII was measured immunocytochemically with the In-Cell Western assay (LI-COR Biosciences). Thirty thousand BHK-M cells expressing wt-fVIII or N1922S-fVIII were plated in 200 μL of DMEM/F12 containing 10% FBS, 100 units/mL penicillin, 100 μg/mL streptomycin, and 100 μg/mL geneticin on a black-walled, clear-bottom, 96-well plate (Greiner Bio-One), grown to confluence overnight, and then switched to serum-free AIM V medium for 24 hours. Cells were fixed in 4% paraformaldehyde, washed 4 times in buffer containing Triton X-100 to permeabilize the cells, and then washed with near-infrared (IR) blocking buffer (Rockland Immunochemicals) for 1 hour at RT. The primary antibody anti-A2 MAb 4A4 was added at a concentration of 1 μg/mL and incubated for 2 hours at RT. After washing 4 times with solution containing 0.2% Tween 20, the secondary antibody, IRDye 800CW goat anti–mouse (LI-COR Biosciences) was diluted in blocking buffer containing 0.2% Tween 20 to a concentration of 1.7 μg/mL, and incubated with the cells for 1 hour at RT. The DRAQ5 nuclear stain (Biostatus Limited) was diluted 1:1000 in DPBS and incubated with the cells for 10 minutes at RT. The cells were washed 4 times with DPBS and imaged using a LI-COR Odyssey 510 Infrared Imaging System set at 800 nm for the secondary antibody and 690 nm for the nuclear stain. The focus offset was at 3 mm and the image intensity was set to 4 for both channels. Quantitation of fVIII was done using the In-Cell Western Analysis plug-in for the Odyssey Infrared Imaging System Application Software v2.1 (LI-COR Biosciences). The 800-nm signal (corresponding to fVIII) was normalized to the 700-nm signal (corresponding to the nuclear stain) to account for differences in total cell number between wt-fVIII and N1922S-fVIII wells. The wt-fVIII wells were set as the 100% standard. Integrated intensity of the fVIII signal in the 800-nm channel was reported for N1922S-fVIII and wt-fVIII.

Immunofluorescence microscopy

Approximately 25 000 naive, wt-fVIII, or N1922S-fVIII BHK-M cells were plated on 8-well collagen-coated culture slides (BD Biosciences) in DMEM/F12 containing 10% FBS, 100 units/mL penicillin, 100 μg/mL streptomycin, and 100 μg/mL geneticin, grown overnight, then switched to serum-free AIMV medium for 24 hours. Cells were washed once with PBS and fixed in 3.7% formaldehyde for 15 minutes. After washing twice with PBS, the cells were permeabilized with 5 washes of 0.1% Triton X-100. After washing once with PBS, Image-iT FX Signal Enhancer (Invitrogen) was added and incubated for 30 minutes at RT. The cells were washed once with PBS, blocked with near-IR blocking buffer for 1 hour, and incubated

with 50 μg/mL of the Golgi probe wheat germ agglutinin–Alexa Fluor 350 conjugate (Invitrogen) for 10 minutes at RT. After washing twice with PBS, the cells were incubated with 1 μg/mL anti-A2 MAb 2-54 and 2.25 μg/mL of the ER probe polyclonal rabbit anti–BiP antibody (Abcam) for 2 hours at RT. After washing 4 times in 0.1% Tween 20 and incubation with 10 μg/mL of the secondary antibodies DyLight 488 donkey anti–mouse and DyLight 549 donkey anti–rabbit (Jackson ImmunoResearch Laboratories) for 1 hour, the cells were washed 4 times with 0.1% Tween 20 and once with PBS, and incubated with 1 mg/mL RNase A for 10 minutes at 37°C. After washing twice with PBS and adding 20μM concentration of the nuclear stain DRAQ5 for 5 minutes, the cells were washed twice with PBS, ProLong-Gold anti-fade reagent (Invitrogen) was added, and the cells were stored overnight in the dark. Images were captured with a Nikon Eclipse Ti inverted microscope using a 60× oil-immersion lens. Image processing was done using NIS Elements AR 3.0 (Nikon Instruments). Exposure times were optimized and the same settings and processing were used for all samples.

Competition ELISA of anti-fVIII antibodies

Costar half-area ELISA plates (Corning) were coated with 6 μg/mL purified MAbs in PBS/0.05% sodium azide, pH 7.4, overnight at 4°C, and then blocked for 2 hours with 2% BSA in HBS/2mM $CaCl_2$/0.05% Tween 20/0.05% sodium azide, pH 7.4. Full-length human fVIII (0.1 μg/mL) was added for 1 hour at RT, followed by the addition of 3 μg/mL biotinylated MAb for 1 hour. Wells were developed by adding streptavidin-alkaline phosphatase conjugate for 1 hour, followed by the addition of *p*-nitrophenylphosphate and measurement of A_{405}, as described previously.[19] Competing and noncompeting MAb pairs were scored by visual inspection of the microtiter wells.

FVIII immunoblotting

Biotrace NT nitrocellulose membranes (Gelman Sciences) were prewetted with HBS for 10 minutes, applied to a dot-blot apparatus (Bio-Rad), and kept hydrated with HBS. wt-fVIII (200 μg/mL in HBS) was either denatured in 1% sodium dodecyl sulfate (SDS), 5% glycerol, 0.062M Tris-Cl, pH 6.8, at 100°C for 5 minutes, or left untreated (native fVIII), followed by the addition of 1 μL per well under vacuum. The membrane was allowed to dry and then blocked with 0.3 mL of near-IR blocking buffer. Primary antibodies were diluted to 1 μg/mL, and 0.1 mL was added to each well. The wells were allowed to drain by gravity, followed by washing 4 times with 0.2 mL of HBS and 0.1% Tween 20, and removal of solution by vacuum. Goat anti–mouse IR conjugate (LI-COR) was diluted 1:10 000 in 1:1 near-IR blocking buffer/0.1% Tween 20, and 0.1 mL was added to each well and allowed to drain by gravity. Wells were washed 4 times with HBS/0.1% Tween 20 and with 0.1 mL of HBS for 5 minutes. Bound goat anti–mouse IR conjugate was detected using a LI-COR Odyssey infrared imaging system.

Structural analysis

Swiss Pdb Viewer Version 4.0.1 was used to study the N1922 mutation site in the 3.70 Å X-ray structure described by Shen et al[9] (PDB ID 2R7E, modified February 24, 2009) and the 3.98 Å X-ray structure described by Ngo et al[10] (PDB ID 3CDZ, modified February 24, 2009). Images were rendered for publication using POV-Ray for Windows Version 3.6.

Results

Hemophilia A due to a N1922S substitution in fVIII

In a recent case-control study, patients with mild to moderate hemophilia and an A3 domain N1922S substitution showed a trend to higher development of inhibitory antibodies to fVIII (inhibitors).[26] The A1, A2, and A3 domains in fVIII possess a pseudo-3-fold axis of symmetry in which the 2 cupredoxin-like subdomains of each domain interface with each other and also form the

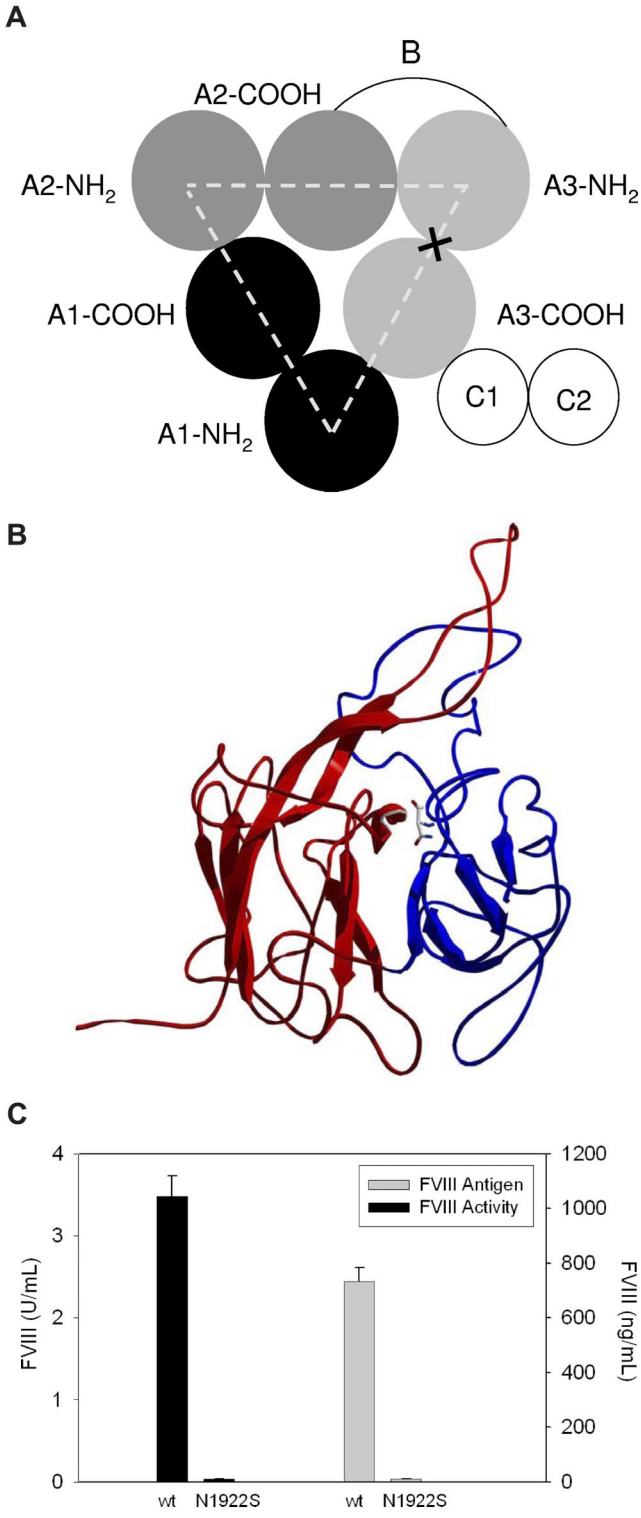

Figure 1. Heterologous expression of N1922S fVIII and wt-fVIII by BHK-M cells. (A) Domain structure of fVIII. X marks the site of the N1922S substitution. (B) Substitution site in N1922S-fVIII. The NH_2-terminal and COOH-terminal subdomains are shown in red and blue, respectively. The N1922 backbone and side chain are shown at the interface of the 2 domains using CPK coloring. (C) BHK-M cells were stably transfected with a plasmid encoding a geneticin-resistance gene and either the N1922S or wt-fVIII cDNA, as described in "Methods." The top N1922S-fVIII clone and a stock wt-fVIII clone were grown to greater than 90% confluence. FVIII activity was measured by one-stage coagulation assay 24 hours after switching to serum-free medium. FVIII antigen also was measured at 24 hours by indirect ELISA using an anti-A2 domain MAb, 4A4, and a biotinylated anti-C2 MAb, 2-117, as capture and detection antibodies, respectively. Results are reported as mean and sample standard deviation of 6 samples per construct.

interdomain A1-A2, A2-A3, A3-A1, and A3-C1 interfaces (Figure 1A). Examination of the available X-ray structures of BDD human fVIII reveals that N1922 lies at the interface of the 2 A3 subdomains (Figure 1B). Solvent-exposure analysis indicates that greater than 99% of the available surface area of N1922 is buried at the interface of the A3 subdomains (data not shown), and thus would not be expected to provide an antibody target. Instead, fVIII inhibitor development in these patients appears to result from an inability to produce sufficient amounts of fVIII antigen to generate immunologic tolerance.

We identified a patient with the N1922S substitution and moderate hemophilia A who developed a fVIII inhibitor that peaked at 32 Bethesda units per milliliter and was associated with intense fVIII exposure surrounding hip replacement surgery. The fVIII level was less than 1%, indicating that the inhibitor cleared the patient's own fVIII as well as wt-fVIII and was directed against epitope(s) remote from the mutation site. After resolution of the inhibitor by immune tolerance induction therapy, the fVIII activity level was 0.017 U/mL and the fVIII antigen level was below the detectable range (< 4 ng/mL). Given the lower limit of detection of the ELISA (4 ng/mL), the specific activity of the patient's fVIII was at least 0.017 U/4 ng or 4300 U/mg. Because the specific activity of wt-fVIII is $\sim$ 4700 U/mg,[27] this indicates that the patient produces a functionally normal fVIII molecule that is secreted poorly.

Heterologous expression of N1922S-fVIII

To determine whether there is a secretion defect associated with N1922S-fVIII, a cDNA encoding BDD N1922S-fVIII was constructed. The expression of N1922S-fVIII contained in a plasmid encoding geneticin resistance from BHK-M cells in serum-free medium was compared with BDD wt-fVIII. Ninety-six geneticin-resistant N1922S-fVIII clones were selected and assayed for fVIII activity and antigen levels. The best N1922S-fVIII clones produced barely detectable levels of fVIII activity and antigen. In contrast, the activity and antigen levels of a stock wt-fVIII clone were 3.5 U/mL and 700 ng/mL, respectively (Figure 1C), similar to previous results with this construct.[23] As a control, we compared the expression of N1922S-fVIII with V634M-fVIII. A V634M substitution in the fVIII A2 domain results in severe CRM-positive hemophilia A due to the secretion of a dysfunctional molecule that circulates at supranormal antigen levels.[28] The activity and antigen levels of V634M-fVIII expressed in BHK-M cells were 0.01 U/mL and 250 ng/mL, respectively (data not shown). This result is consistent with the clinical phenotype and similar to heterologous expression of V634M-fVIII in Chinese hamster ovary cells.[16]

In some expression systems, the presence of serum results in increased extracellular fVIII levels due to the stabilization of fVIII by VWF in the serum.[29] However, the expression of N1992S also was barely detectable in medium containing 10% FBS (data not shown), indicating that the expression defect associated with the N1922S substitution is due to a block in intracellular transport and not an inability to bind and be stabilized by VWF.

Intracellular expression of N1922S-fVIII

Intracellular expression of fVIII in BHK-M cells was measured immunocytochemically with the In-Cell Western assay using an anti-A2 MAb, 4A4, as the primary antibody. MAb 4A4 recognizes a linear-immunodominant epitope bounded by residues R484 and I508[19] that projects from 2 β strands in the fVIII A2 domain.[9,10] MAb 4A4 was selected because in immunoblotting assays it binds to fVIII that has been denatured by heating in SDS (results not shown), which is consistent with the fact that it recognizes a linear epitope. Thus, 4A4 potentially recognizes intracellular fVIII polypeptide in both folded and nonfolded states. wt-fVIII and N1922S-fVIII BHK-M cells produced indistinguishable images using this method (data not shown). Furthermore, densitometric quantitation of intracellular fVIII expression yielded no significant difference between wt-fVIII and N1922S-fVIII (Figure 2).

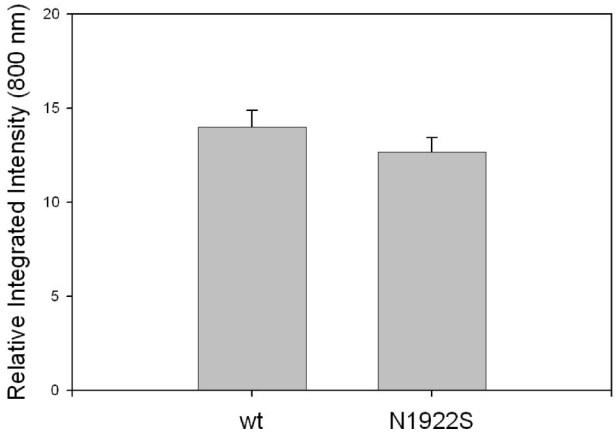

Figure 2. Intracellular expression of wt-fVIII and N1922S-fVIII in BHK-M cells. Confluent monolayers of BHK-M cells expressing wt-fVIII or N1922S-fVIII were permeabilized with Triton X-100 and incubated with the anti-A2 MAb 4A4. After washing, the cells were incubated with goat anti–mouse IRDye 800CW secondary antibody. Infrared fluorescence emission of the secondary antibody was detected at 800 nm and quantitated densitometrically as described in "Immunocytochemical assay of fVIII." Results are reported as mean and sample standard deviation (n = 4 per construct).

Subcellular localization of wt-fVIII and N1922S-fVIII

FVIII follows the so-called classic secretory pathway that includes translocation of the nascent polypeptide chain to the ER, where folding occurs, followed by transit to the Golgi for further processing, and finally packaging into post–Golgi-transport intermediates that move through the cytoplasm to the cell surface.[30,31] To determine where the secretory pathway is blocked during the expression of N1922S-fVIII, we performed immunofluorescence microscopy using an anti-A2 antibody 2-54, the ER-specific probe BiP, and the Golgi probe wheat germ agglutinin (Figure 3). Overall expression of wt-fVIII and N1922S-fVIII were similar, consistent with In-Cell Western analysis. In addition, both wt-fVIII and N1922S-fVIII colocalized to the ER with BiP (Figure 3A). However, only wt-fVIII colocalized to Golgi with wheat germ agglutinin (Figure 3B). This result demonstrates that folding of N1922S-fVIII is stalled in the ER, preventing or delaying its transport to the Golgi and subsequently limiting its secretion from the cell.

Functional characterization of intracellular and extracellular wt-fVIII and N1922S-fVIII

To compare the maturation of wt-fVIII and N1922S-fVIII into functional, folded states during cellular expression, the specific activities of their secreted and intracellular forms were determined using fVIII antigen measurement as an estimate of mass (Figure 4). Although secreted N1922S-fVIII activity was very low at 0.04 U/mL (Figure 1C), its specific activity was comparable with wt-fVIII (2800 vs 4800 U/mg). Given the low concentrations of N1922S-fVIII in the medium, the modest decrease in specific activity was possibly due to partial denaturation in dilute medium rather than a true functional difference from wt-fVIII. In addition,

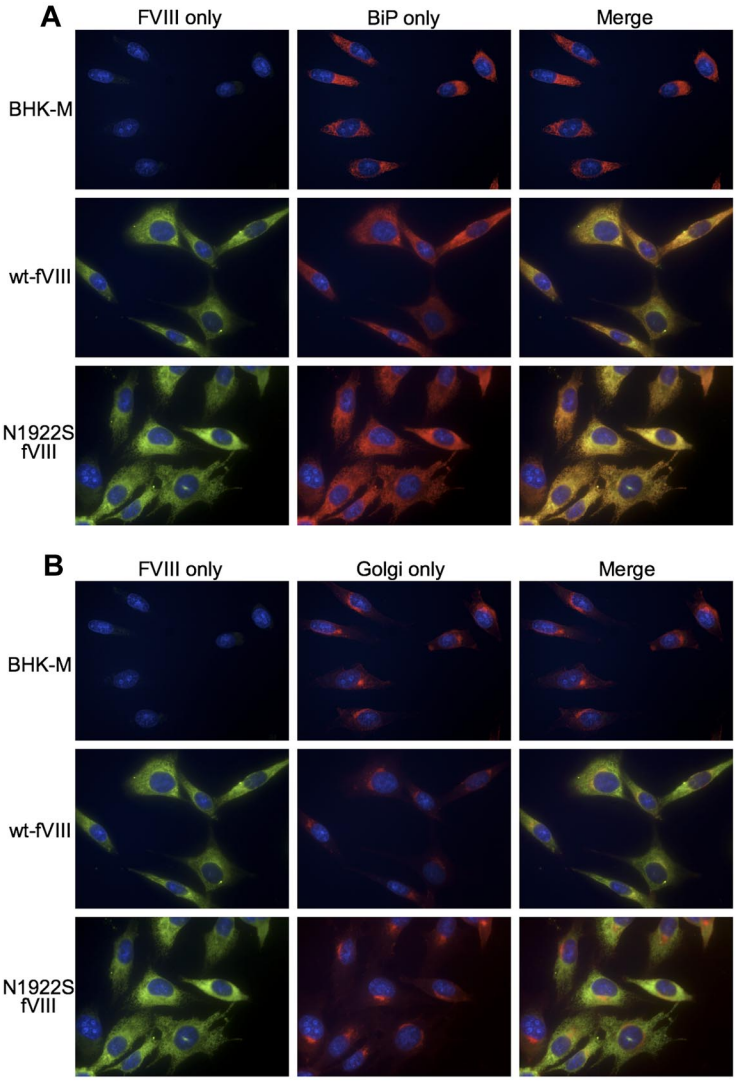

Figure 3. Immunofluorescence microscopy of BHK-M cells expressing wt-fVIII and N1922S-fVIII. BHK-M cells, BHK-M cells expressing wt-fVIII, or BHK-M cells expressing N1922S-fVIII were incubated with anti-A2 MAb 2-54, ER probe polyclonal rabbit anti-BiP antibody (A) and the Golgi probe wheat germ agglutinin–Alexa Fluor 350 conjugate (B). The primary antibodies were detected with DyLight 488 donkey anti–mouse and DyLight 549 donkey anti–rabbit secondary antibodies. Nuclear staining was performed using DRAQ5. Images were captured with a Nikon Eclipse Ti inverted microscope using a 60× oil-immersion lens.

the activation quotients of wt-fVIII and N1922S-fVIII, which measure the ability of thrombin to activate fVIII, were similar. The specific activities of secreted and intracellular wt-fVIII were similar. However, the specific activity of intracellular N1922S-fVIII was only ~10% of secreted N1922S-fVIII (290 vs 2800 U/mg).

A plasma-free intrinsic fXase assay also was used to compare the thrombin activation of secreted and intracellular wt-fVIII and N1922S-fVIII using purified wt-fVIII as the positive control. Secreted wt-fVIII and N1922S-fVIII had specific activities within 5% of purified wt-fVIII. In contrast, intracellular N1922S-fVIII had less than 5% of the specific activity of purified wt-fVIII (data not shown). Intracellular wt-fVIII had twice the specific activity of the control wt-fVIII, suggesting minor proteolytic activation during the lysis process. These results are consistent with the phenotype of the hemophilia A N1922S patient, and indicate that the mutation results in poor secretion of a functionally normal or near normal fVIII molecule.

Characterization of domain-specific anti-fVIII antibodies as probes of fVIII folding

The low specific activity of intracellular N1922S-fVIII indicates that at least one step along its folding pathway is stalled, leading to the accumulation of an inactive intermediate in the ER with inability to transit to the Golgi. To probe the folded, tertiary structure of intracellular fVIII, we used a panel of domain-specific anti-fVIII MAbs. Antibodies raised to native, fully folded proteins usually are conformation specific and recognize discontinuous sequences in the folded polypeptide chain.[32] Antigen recognition of the corresponding partially folded or denatured protein is usually decreased or lost.

Because we were particularly interested in the structure of the mutated A3 domain, we first surveyed a panel of 6 anti-A3 MAbs to identify groups of nonoverlapping antibodies. FVIII was bound in a sandwich ELISA to an immobilized anti-A3 capture MAb, and the binding of a second biotinylated anti-A3 MAb was evaluated. Binding of the secondary MAb indicates that its epitope is nonoverlapping with the capture MAb, whereas the absence of binding indicates the presence of overlapping epitopes. A matrix showing the competition pattern of the MAbs is shown in Figure 5A. Noncompeting and competing MAbs are depicted as color (gray) or white producing elements, respectively. The diagonal elements are white, indicating that each MAb competed with itself for binding, as expected. In addition, the matrix is symmetric, demonstrating that the same results were obtained regardless of the configuration of the MAb pairs. Thus, there was no loss of binding

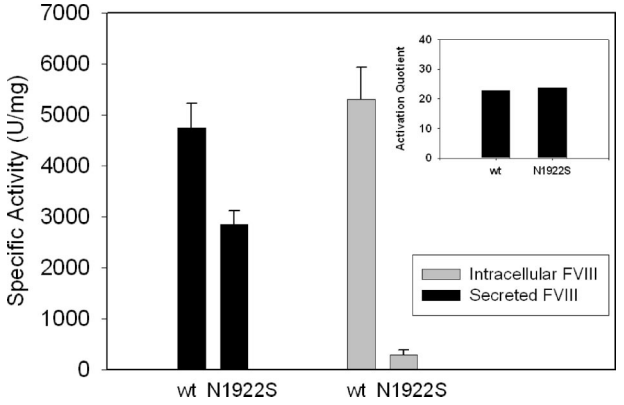

Figure 4. Functional characterization of secreted and intracellular wt-fVIII and N1922S-fVIII. BHK-M cells expressing wt-fVIII or N1922S-fVIII were switched to serum-free medium for 24 hours, followed by removal of the medium and extraction of intracellular fVIII from cell lysate, as described in "Heterologous expression of fVIII." Specific activity of fVIII secreted into the medium or intracellular fVIII was determined as the ratio of fVIII activity measured by one-stage coagulation assay to fVIII antigenic mass measured by ELISA. The inset shows the activation quotients of wt-fVIII and N1922S-fVIII in the medium.

due to biotinylation of the antigen-binding site of the antibody or other anomalous behavior. The matrix reveals that MAbs I143, 2-113, I92, and I130 form one group that does not overlap with a second group consisting of F147 and G38.

The ability of a panel of domain-specific MAbs, including these anti-A3 MAbs, to recognize native wt-fVIII or denatured wt-fVIII produced by heating in 1% SDS was evaluated by immunoblotting analysis. Binding was quantitated by measuring the fluorescence of bound secondary anti–mouse antibody. Figure 5B shows that the ratio of denatured fVIII to native fVIII binding by 2-116 (anti-A1), 1D4 (anti-A2), 2-113 (anti-A3), 2A9 (anti-C1), 3E6 (anti-C2), and 2-117 (anti-C2) MAbs was less or equal to 0.1, indicating that folding and tertiary structure formation is necessary for recognition by these MAbs. Thus, conformation-specific MAbs to all of the fVIII domains were available for analysis. Two additional anti-A3 MAbs, I92 and G38, bound significantly to denatured fVIII, indicating that they are less conformationally dependent.

Binding of intracellular and secreted fVIII to conformation-specific, domain-specific antibodies

The concentration of an analyte such as fVIII can be estimated by ELISA using a standard curve constructed using purified analyte. If a test analyte binds an antibody used in the ELISA less than the standard curve analyte, then its apparent concentration will be lower than the true concentration. Thus, for a given anti-fVIII ELISA antibody and a standard curve using wt-fVIII, an underestimate of the concentration of N1922S-fVIII indicates that the domain recognized by the antibody is not in the native, folded state.

We used this approach to evaluate the folding of individual domains of secreted and intracellular wt-fVIII and N1922S-fVIII. MAb 4A4, which recognizes denatured and native fVIII, was used to capture wt-fVIII or N1922S-fVIII from BHK-M medium and cell lysates, which was followed by the addition of the domain-specific biotinylated test MAbs, as described in Figure 5A. Because the intracellular levels of total wt-fVIII and N1922S fVIII estimated using MAb 4A4 for detection were similar (Figure 2), any decrease in the apparent concentrations of N1922S-fVIII using this method indicates poor binding by the test MAbs. There was relatively little variation among the 8 test MAbs with respect to either secreted or intracellular wt-fVIII (Figure 6A). The lack of variation for intracellular fVIII indicates that the native, fully folded wt-fVIII is the dominant species that was detected. In contrast to wt-fVIII, the apparent intracellular concentrations of N1922S-fVIII varied widely among the test MAbs (Figure 6B), and were lowest among the conformation-specific MAbs, anti-A3 MAb and 2-113, and the anti-C1 MAb, 2A9. The domain-specific folding of wt-fVIII and N1922S-fVIII was compared by calculating the ratios of intracellular-to-secreted wt-fVIII and N1922S-fVIII (Figure 6C). There was relatively little variation in the wt-fVIII ratios, indicating no conformational differences between intracellular and secreted wt-fVIII. However, there was wide variation in the N1922S-fVIII ratios, with the anti-C2 MAbs displaying the highest ratios and the anti-A3 MAbs and anti-C1 MAb the lowest ratios. Although the anti-A3 MAbs I92 and G38 recognized SDS-denatured N1922S-fVIII (Figure 5B), they recognized intracellular N1922S poorly. This indicates that SDS only partially denatures

A

	I143	2-113	I92	I130	F147	G38	Epitope
I143							1818-1916
2-113							1818-1916
I92							1818-1916
I130							1818-1916
F147							1690-1817
G38							1690-1817

B

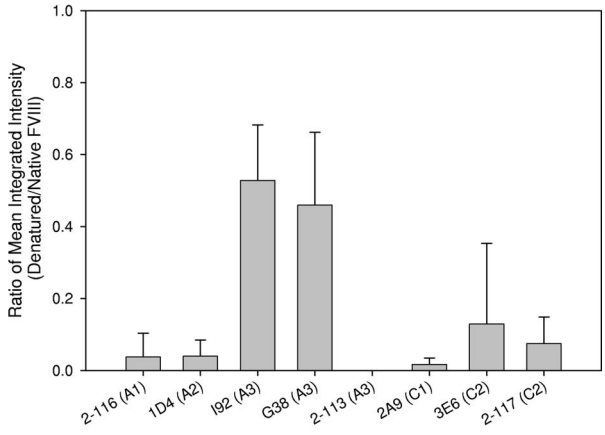

Figure 5. Characterization of domain-specific anti-A3 MAbs. (A) Overlapping epitopes recognized by anti-A3 MAbs were identified by competition ELISA. Human fVIII was bound to MAbs I143, 2-113, I92, I130, F147, or G38 that were immobilized to microtiter wells. Corresponding biotinylated MAbs were added and binding was detected using streptavidin-alkaline phosphatase conjugate. The rows and columns correspond to unmodified, immobilized MAbs, and solution-phase, biotinylated MAbs, respectively. Epitopes recognized by MAbs were mapped as described in supplemental Figure 1. (B) Native wt-fVIII or wt-fVIII were denatured by heating in SDS and adsorbed to nitrocellulose membranes, followed by the addition of the indicated domain-specific murine anti-fVIII MAb and goat anti–mouse IR conjugate. The ratio of fluorescence of goat anti–mouse IR conjugate bound to denatured fVIII versus wt-fVIII was determined using a LI-COR Odyssey infrared imaging system. Results are reported as mean and sample standard deviation of triplicate samples for each MAb.

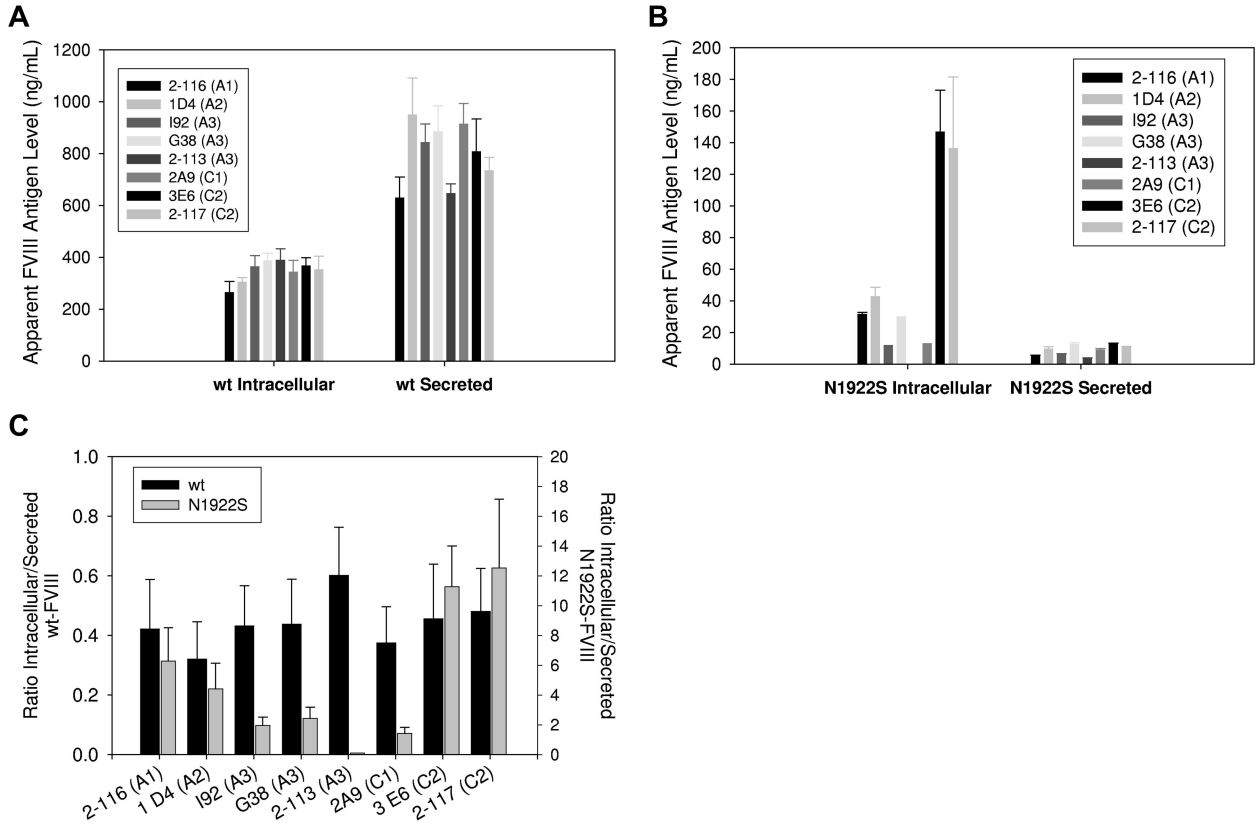

Figure 6. Antigenic characterization of secreted and intracellular wt-fVIII and N1922S-fVIII. Anti-A2 MAb 4A4 was used to capture secreted and intracellular wt-fVIII and N1922S-fVIII from BHK-M medium and cell lysates, respectively. The binding of biotinylated secondary MAbs 2-116 (anti-A1), 1D4 (anti-A2), I92 (anti-A3), G38 (anti-A3), 2-113 (anti-A3), 2A9 (anti-C1), 3E6 (anti-C2), or 2-117 (anti-C2) was measured colorimetrically, as described in "Methods." Apparent antigen levels for wt-fVIII (A) and N1922S-fVIII (B) were calculated by means of a standard curve using purified wt-fVIII of 2 to 8 samples per construct. (C) The ratio of apparent intracellular antigen to secreted antigen was calculated from the results shown in panels A and B.

the epitopes recognized by these MAbs, which are poorly developed in intracellular N1922S fVIII, or that misfolding in the A3 domain buries the linear epitopes, making them inaccessible. There was a relatively modest decrease in the ratios observed for the anti-A1 and anti-A2 MAbs compared with the anti-C2 MAbs. Overall, the results shown in Figure 6 identify the presence of an N1922S-fVIII intermediate in which the mutated A3 domain and the adjacent C1 domain are stalled in an unfolded state.

Discussion

Biosynthetic defects associated with point mutations or small deletions/insertions in the *F8* gene that lead to undetectable fVIII antigen (CRM-negative hemophilia A) have not been extensively characterized. Using a heterologous expression system, Amano et al observed hyposecretion of an fVIII A2-domain deletion mutant, DeltaF652/3.[16] In addition, Roelse et al found that R593C and N618S A2-domain substitutions led to elevated accumulation of intracellular functional fVIII relative to wt-fVIII.[33] In these studies, the kinetic block in fVIII synthesis was not identified.

In the present study, we used conformation-specific MAbs, which have been used as tools to study protein folding, including intracellular folding intermediates,[34] to detect folding intermediates in the biosynthesis of wt-fVIII and N1922S-fVIII. An intermediate containing incompletely folded A3 and C1 domains was identified after measurement of the apparent ratios of intracellular to secreted N1922S-fVIII (Figure 6C). N1922 in the COOH-terminal A3 subdomain is buried at the interface with the NH_2-terminal subdomain (Figure 1B). In both X-ray structures of fVIII, N1922 is tightly packed against and hydrogen bonded to F1879 in the NH_2-terminal subdomain. Our results suggest that the N1922S substitution produces a kinetic defect in the folding of the A3 domain, which stalls fVIII synthesis, although ultimately the fVIII that is secreted is normal or near normal.

In the X-ray structures of BDD fVIII, the A3 domain forms an extensive hydrophobic interface with the C1 domain, indicating that the A3-C1 structure is fixed and nonflexible.[9,10] This is consistent with our finding that the N1922S A3 domain substitution also interferes with folding of the C1 domain. In contrast, the C2 domain, which, like the C1 domain, is COOH-terminal and downstream of A3 domain synthesis, appears to be normally folded in this intermediate. Unlike the C1 domain, the C2 domain does not have an extensive hydrophobic interface and is loosely tethered,[9] and thus evidently folds independently of the A3 domain.

The concentration of fVIII in human plasma (0.1-0.2 μg/mL) is lower than all of the other clotting factors.[35] The plasma concentration of fVIII is tightly controlled and apparently is a limiting factor in fibrin clot formation, because an increase of only 1.5× normal is associated with venous and arterial thromboembolism.[36-39] Consistent with these low plasma levels, the secretion of fVIII from primary endothelial cell cultures is barely detectable.[4-6] In addition, the heterologous expression of fVIII in mammalian cell culture typically is at least 100-fold lower than that observed with other genes.[30] Comparing the expression of fVIII and factor V (fV) is of particular interest because fV is homologous to fVIII and contains

an A1-A2-B-A3-C1-C2 domain structure.[40,41] The secretion of fVIII is more than 100-fold lower than fV, which is consistent with the 50-fold lower plasma levels of fVIII. This difference is primarily due to inefficient transport of fVIII out of the ER compared with fV. Unlike fV, fVIII associates with the molecular chaperone BiP, which binds exposed hydrophobic patches of incompletely folded proteins. In contrast to fV, a large fraction of fVIII never exits the ER and is degraded in the proteasome. There are significant interspecies differences in fVIII expression. The heterologous expression of porcine BDD fVIII is at least 10-fold greater than human BDD fVIII,[23] which is consistent with the higher levels of fVIII in porcine plasma compared with human plasma. Heterologous expression of hybrid human fVIII that contains the porcine A1 and A3 domains is comparable with that of porcine fVIII due to increased secretion efficiency.[42]

The relative secretion efficiencies of wt-fVIII versus N1922S-fVIII, fV versus fVIII, and porcine fVIII versus human fVIII result from differential rates of transit of the polypeptide chain from the ER to the Golgi. ER-to-Golgi transport generally is considered rate limiting in secretion of intracellular proteins.[43] This process involves folding of the nascent polypeptide chain and then transport by cargo proteins that differentially bind the secretory proteins and carry them to the Golgi in vesicular carriers through the ER-Golgi intermediate compartment. For example, mutations in the ER-Golgi intermediate compartment cargo proteins LMAN1 or MCFD2 produce the autosomal recessive disorder combined fV/fVIII deficiency.[44,45]

The increased secretion efficiency of porcine fVIII versus wt-fVIII is controlled by the A1 and A3 domains. Improper folding in the A3 domain leads to poor secretion of N1922S-fVIII. Thus, in addition to transport rates from the ER to the Golgi, fVIII expression levels are dependent on proper folding of the polypeptide chain. These results demonstrate that folding of the A domains specifically is rate determining in the secretion of fVIII.

Acknowledgments

This study was supported by National Institutes of Health (NIH) grant K08 HL102262 and Hemophilia of Georgia Inc (to S.L.M.); by NIH grants R01 HL 092179 (to C.B.D.); and by NIH grants R01 HL082609 and R01 HL040921 and Hemophilia of Georgia Inc (to P.L.).

Authorship

Contribution: R.J.S., S.L.M., J.F.H., H.C.B., and E.T.P. designed and performed research, analyzed data, and cowrote the paper; and C.L.K., C.B.D., and P.L. designed research, analyzed data, and cowrote the paper.

Conflict-of-interest disclosure: The authors declare no competing financial interests.

Correspondence: Pete Lollar, MD, Emory Children's Center, Rm 426D, 2015 Uppergate Dr, Atlanta, GA 30322; e-mail: jlollar@emory.edu.

References

1. White GC II, Rosendaal F, Aledort LM, et al; Factor VIII and Factor IX Subcommittee. Definitions in hemophilia. Recommendation of the scientific subcommittee on factor VIII and factor IX of the scientific and standardization committee of the International Society on Thrombosis and Haemostasis. *Thromb Haemost.* 2001;85(3):560.
2. Franchini M, Favaloro EJ, Lippi G. Mild hemophilia A. *J Thromb Haemost.* 2010;8(3):421-432.
3. Wion KL, Kelly D, Summerfield JA, Tuddenham EG, Lawn RM. Distribution of factor VIII mRNA and antigen in human liver and other tissues. *Nature.* 1985;317(6039):726-729.
4. Do H, Healey JF, Waller EK, Lollar P. Expression of factor VIII by murine liver sinusoidal endothelial cells. *J Biol Chem.* 1999;274(28):19587-19592.
5. Jacquemin M, Neyrinck A, Hermanns MI, et al. FVIII production by human lung microvascular endothelial cells. *Blood.* 2006;108(2):515-517.
6. Shahani T, Lavend'homme R, Luttun A, et al. Activation of human endothelial cells from specific vascular beds induces the release of a FVIII storage pool. *Blood.* 2010;115(23):4902-4909.
7. Lenting PJ, van Schooten CJ, Denis CV. Clearance mechanisms of von Willebrand factor and factor VIII. *J Thromb Haemost.* 2007;5(7):1353-1360.
8. Pemberton S, Lindley P, Zaitsev V, et al. A molecular model for the triplicated A domains of human factor VIII based on the crystal structure of human caeruloplasmin. *Blood.* 1997;89(7):2413-2421.
9. Shen BW, Spiegel PC, Chang C-H, et al. The tertiary structure and domain organization of coagulation factor VIII. *Blood.* 2008;111(3):1240-1247.
10. Ngo JC, Huang M, Roth DA, Furie BC, Furie B. Crystal structure of human factor VIII: implications for the formation of the factor IXa-factor VIIIa complex. *Structure.* 2008;16(4):597-606.
11. Lollar P, Parker CG. Subunit structure of thrombin-activated porcine factor VIII. *Biochemistry.* 1989;28(2):666-674.
12. Lollar P, Parker CG. pH-dependent denaturation of thrombin-activated porcine factor VIII. *J Biol Chem.* 1990;265(3):1688-1692.
13. Jacquemin M, De Maeyer M, d'Oiron R, et al. Molecular mechanisms of mild and moderate hemophilia A. *J Thromb Haemost.* 2003;1(3):456-463.
14. d'Oiron R, Pipe SW, Jacquemin M. Mild/moderate haemophilia A: new insights into molecular mechanisms and inhibitor development. *Haemophilia.* 2008;14(suppl 3):138-146.
15. Jacquemin M, Lavend'homme R, Benhida A, et al. A novel cause of mild/moderate hemophilia A: mutations scattered in the factor VIII C1 domain reduce factor VIII binding to von Willebrand factor. *Blood.* 2000;96(3):958-965.
16. Amano K, Sarkar R, Pemberton S, et al. The molecular basis for cross-reacting material-positive hemophilia A due to missense mutations within the A2-domain of factor VIII. *Blood.* 1998;91(2):538-548.
17. Pipe SW, Eickhorst AN, McKinley SH, Saenko EL, Kaufman RJ. Mild hemophilia A caused by increased rate of factor VIII A2 subunit dissociation: evidence for nonproteolytic inactivation of factor VIIIa in vivo. *Blood.* 1999;93(1):176-183.
18. Funk WD, MacGillivray RT, Mason AB, Brown SA, Woodworth RC. Expression of the amino-terminal half-molecule of human serum transferrin in cultured cells and characterization of the recombinant protein. *Biochemistry.* 1990;29(6):1654-1660.
19. Healey JF, Parker ET, Barrow RT, et al. The humoral response to human factor VIII in hemophilia A mice. *J Thromb Haemost.* 2007;5(3):512-517.
20. Lind P, Larsson K, Spira J, et al. Novel forms of B-domain-deleted recombinant factor VIII molecules. Construction and biochemical characterization. *Eur J Biochem.* 1995;232(1):19-27.
21. Healey JF, Barrow RT, Tamim HM, et al. Residues Glu2181-Val2243 contain a major determinant of the inhibitory epitope in the C2 domain of human factor VIII. *Blood.* 1998;92(10):3701-3709.
22. Horton RM, Ho SN, Pullen JK, et al. Gene splicing by overlap extension. *Methods Enzymol.* 1993;217:270-279.
23. Doering CB, Healey JF, Parker ET, Barrow RT, Lollar P. High-level expression of recombinant porcine coagulation factor VIII. *J Biol Chem.* 2002;277(41):38345-38349.
24. Lollar P, Parker ET, Fay PJ. Coagulant properties of hybrid human/porcine factor VIII molecules. *J Biol Chem.* 1992;267(33):23652-23657.
25. Parker ET, Doering CB, Lollar P. A1 subunit-mediated regulation of thrombin-activated factor VIII A2 subunit dissociation. *J Biol Chem.* 2006;281(20):13922-13930.
26. Kempton CL, Soucie JM, Miller CH, et al. In non-severe hemophilia A the risk of inhibitor following intensive factor treatment is greater in older patients: a case-control study. *J Thromb Haemost.* 2010;8(10):2224-2231.
27. Rotblat F, O'Brien DP, O'Brien FJ, Goodall AH, Tuddenham EGD. Purification of human factor VIII:C and its characterization by Western blotting using monoclonal antibodies. *Biochemistry.* 1985;24(16):4294-4300.
28. McGinniss MJ, Kazazian HH, Jr, Hoyer LW, et al. Spectrum of mutations in CRM-positive and CRM-reduced hemophilia A. *Genomics.* 1993;15(2):392-398.
29. Kaufman RJ, Wasley LC, Dorner AJ. Synthesis, processing, and secretion of recombinant human factor VIII expressed in mammalian cells. *J Biol Chem.* 1988;263(13):6352-6362.
30. Kaufman RJ, Pipe SW, Tagliavacca L, Swaroop

M, Moussalli M. Biosynthesis, assembly and secretion of coagulation factor VIII. *Blood Coagul Fibrinolysis.* 1997;8(suppl 2):S3-S14.

31. Becker S, Simpson JC, Pepperkok R, et al. Confocal microscopy analysis of native, full length and B-domain deleted coagulation factor VIII trafficking in mammalian cells. *Thromb Haemost.* 2004;92(1):23-35.
32. Davies DR, Cohen GH. Interactions of protein antigens with antibodies. *Proc Natl Acad Sci U S A.* 1996;93(1):7-12.
33. Roelse JC, de Laaf RTM, Timmermans SMH, et al. Intracellular accumulation of factor VIII induced by missense mutations Arg593 → Cys and Asn(618) → Ser explains cross-reacting material-reduced haemophilia A. *Br J Haematol.* 2000; 108(2):241-246.
34. Francis E, Daniels R, Hebert DN. Analysis of protein folding and oxidation in the endoplasmic reticulum. *Curr Protoc Cell Biol.* 2002;Chapter 15: Unit 15.6
35. Monroe DM, Hoffman M, Roberts HR. Molecular biology and biochemistry of the coagulation factors and pathways of hemostasis. In: Kaushansky K, Lichtman MA, Beutler E, Kipps TJ, Selighsohn U, Prchal JT, eds. Williams hematology. New York: McGraw Hill; 2010:1815-1843.
36. Brandt JT. Measurement of factor VIII. A potential risk factor for vascular disease. *Archi Pathol Lab Med.* 1993;117(1):48-51.
37. Kraaijenhagen RA, in't Anker PS, Koopman MM, et al. High plasma concentration of factor VIIIc is a major risk factor for venous thromboembolism. *Thromb Haemost.* 2000;83(1):5-9.
38. Kyrle PA, Minar E, Hirschl M, et al. High plasma levels of factor VIII and the risk of recurrent venous thromboembolism. *N Engl J Med.* 2000;343(7): 457-462.
39. Kamphuisen PW, Eikenboom JC, Bertina RM. Elevated factor VIII levels and the risk of thrombosis. *Arterioscler Thromb Vasc Biol.* 2001;21(5): 731-738.
40. Pittman DD, Tomkinson KN, Kaufman RJ. Post-translational requirements for functional factor V and factor VIII secretion in mammalian cells. *J Biol Chem.* 1994;269(25):17329-17337.
41. Pipe SW, Morris JA, Shah J, Kaufman RJ. Differential interaction of coagulation factor VIII and factor V with protein chaperones calnexin and calreticulin. *J Biol Chem.* 1998;273(14):8537-8544.
42. Doering CB, Healey JF, Parker ET, Barrow RT, Lollar P. Identification of porcine coagulation factor VIII domains responsible for high level expression via enhanced secretion. *J Biol Chem.* 2004; 279(8):6546-6552.
43. Lodish HF, Kong N, Snider M, Strous GJ. Hepatoma secretory proteins migrate from rough endoplasmic reticulum to Golgi at characteristic rates. *Nature.* 1983;304(5921):80-83.
44. Nichols WC, Seligsohn U, Zivelin A, et al. Mutations in the ER-Golgi intermediate compartment protein ERGIC-53 cause combined deficiency of coagulation factors V and VIII. *Cell.* 1998;93(1): 61-70.
45. Zhang B, Cunningham MA, Nichols WC, et al. Bleeding due to disruption of a cargo-specific ER-to-Golgi transport complex. *Nat Genet.* 2003; 34(2):220-225.